Response of ENSO and the Mean State of the Tropical Pacific to Extratropical Cooling/Warming: A Study Using the IAP Coupled Model

Y. Yu[1] and D.-Z. Sun[2,3]

1. LASG, Institute of Atmospheric Physics (IAP), Beijing, China (yyq@lasg.iap.ac.cn /Fax +86 10-82995172)

2. University of Colorado/CIRES & NOAA/ESRL, Boulder, Colorado, USA (dezheng.sun@noaa.gov /Fax +01 303 4976449)

3. School of Human Settlement and Civil Engineering, Xian Jiaotung University, Xian, China

May 30 2009

Abstract

The coupled model of Institute of Atmospheric Physics (IAP) is used to investigate the effects of extratropical cooling/warming on the tropical Pacific climate. The IAP coupled model is a fully coupled GCM without any flux correction. The model has been used in many aspects of climate modeling including the IPCC AR4 climate change and paleo-climate simulations. In this study, we subject the IAP coupled model to cooling or heating over the extratropical Pacific. As in an earlier study, we impose the cooling/heating over the extratropical region poleward of 10^{o}N-10^{o}S.

Consistent with earlier findings, we have found an elevated (reduced) level of ENSO activity in response to an increase (decrease) in the cooling over the extratropical region. We have also found that the changes in the time-mean structure of the equatorial upper ocean are very different between the case in which ocean-atmosphere is coupled over the equatorial region and the case in which the ocean-atmosphere over the equatorial region is decoupled. For example, in the uncoupled run, the thermocline water across the entire equatorial Pacific is cooled in response to an increase in the extratropical cooling. In the corresponding coupled run, the changes in the equatorial upper ocean temperature in the extratropical cooling resemble a La Nina situation—a deeper thermocline in the western and central Pacific accompanied by a shallower thermocline in the eastern Pacific. Conversely, with coupling, the response of the equatorial upper ocean to extratropical cooling resembles an El Nino situation. These results ascertain the role of extratropical ocean in determining the amplitude of ENSO. The results also underscore the importance of ocean-atmosphere coupling in the interaction between the tropical Pacific and the extra-tropical Pacific.

1. Introduction

El Niño Southern Oscillation (ENSO) is a prominent mode of the climate system and affects climate world-wide (Trenberth et al. 1998). Understanding the fundamental forces that control the level of ENSO activity is a basic issue in the study of climate dynamics. While our understanding of many aspects of ENSO is quite advanced (Neelin et al. 1998), the understanding of global factors controlling the level of ENSO activity is still limited (Wang and Picaut 2004, Sun 2004).

Among the global factors that have been suggested to be potentially important in influencing ENSO is the subtropical/extratropical cooling or heating. Using a coupled model, Bush et al. (1998) investigated the impact of extratropical cooling associated with the Last Glacial Maxium on the tropical Pacific SST. They found that the tropical air-sea interaction amplifies the cooling effect from the high latitudes on the tropics. The attributed this amplification to two factors: (1) the positive Bjerknes feedback within the tropics (Neelin et al. 1998) and (2) the exchange of water between the tropics and extratropics through the "ocean tunnel"—surface water of the extratropical ocean is subducted downward and equatorward to feed the equatorial undercurrent and therefore the equatorial upwelling (Pedlosky 1987, Liu et al 1994, McCreary and Lu 1994). They did not analyze, however, the corresponding changes in ENSO amplitude. Using a simple box model, Sun (1997, 2000) suggested that the amplitude of ENSO may depend on the subsurface temperatures and therefore raised the possibility that extratropical/subtropical cooling/warming may influence the amplitude of ENSO as the equatorial thermocline water comes from the extratropical/subtropical ocean. Using a hybrid coupled model—the NCAR Pacific basin model coupled to an empirical atmosphere, Sun et al. (2004) conducted numerical experiments to further investigate the response of the ENSO amplitude to an imposed extratropical cooling/warming. They found that the level of ENSO activity increases in response to an increase in the extratropical cooling. They explain this result by noting that the extratropical cooling eventually cools the equatorial thermocline water and thereby destabilize the coupled equatorial ocean-atmosphere system. The stronger ENSO is a response to this destabilizing forcing. Conversely, they found that an extratropical warming (or a decrease in extratropical cooling) reduces the

level of ENSO activity. Combined with the results from an earlier study on the impact of an increase in the radiative heating over the tropics on the ENSO amplitude (Sun 2003), the results of Sun et al. (2004) links the amplitude of ENSO to the meridional differential heating over the Pacific ocean and thereby to the heat uptake of the tropical Pacific and poleward heat transport from that region. Fedorov et al. (2006) also suggested an important role of extratropical warming/cooling and the poleward heat transport in determining the level of ENSO activity. In particular, they suggested that the apparent lack of ENSO activity 3 million years ago may be a consequence of a much warmer extratropics during that period (Fedorov et al. 2006). In the same vein, they suggest that the subsequent onset of ENSO was a response to the gradual cooling in the extratropics taking place since 3 millions years ago.

Following upon the study of Sun et al. (2004), Sun and Zhang (2006) further showed that the response of the time-mean state of the tropical Pacific to extratropical cooling is very different in the case when the equatorial ocean-atmosphere is coupled (the case with ENSO) and in the case when the equatorial ocean-atmosphere is not coupled. Their results suggest that ENSO has a time-mean effect on the time-mean state. (Specifically, the study of Sun and Zhang (2006) suggests that ENSO events, collectively, may act as a basin-scale heat mixer that prevent the time-mean difference between the warmpool SST and the temperature of the equatorial thermocline water from exceeding a critical value). As suggested by Rodger et al. (2004), Schopf and Burgman (2006), and Sun and Yu (2008), ascertaining and understanding the time-mean effect of ENSO could be critical to a better understanding of the decadal variability in the tropical Pacific

The twin questions raided by aforementioned studies---what is the role of extratropical cooling in determining the amplitude of ENSO and what is the feedback from ENSO on the mean climate of the tropical Pacific---are obviously important for understanding factors outside the tropical Pacific in determining the level of ENSO activity, and more generally for understanding the role of ocean-atmosphere interaction in tropical-extratropical communication in the climate system. The present investigation is to further address these questions. The focus is on understanding, so we take a step-by-step approach by following the methodology used in Sun et al. (2004) closely. We will, however, use a more sophisticated coupled model—both components of the

model are GCMs. The paper is organized as follows. The model and experiment design is discussed in section 2. In section3, we present the main results. Summary and discussion are provided in section 4.

2. Model Description and Experiment Design

The version g1.1 of IAP coupled GCM FGOALS is used in study to investigate the effect of the extra-tropical cooling and warming on ENSO behavior. The coupled GCM consists of four interactive components: atmospheric, oceanic, land and sea ice models connected by NCAR flux coupler version 5 (Collins et al. 2003). The oceanic component model is a LASG/IAP Climate system Ocean Model (LICOM) version1.1 (Zhang et al. 2003; Liu et al. 2004; Xiao and Yu 2006). In this study, the horizontal resolution of LICOM was subscribed to 1.0°×1.0°, and thirty levels are used in vertical with 12 equal levels in the upper 300 meters. The atmospheric component model is a grid-point model: Atmospheric Model of IAP/LASG (GAMIL). The dynamical core includes a finite difference scheme that conserves total mass and energy in solving the primitive hydrostatic equations of a baroclinic atmosphere [Wang et al., 2004], and a two-step shape-preserving advection scheme for the moisture equation (Yu 1994). The model employs a hybrid horizontal grid, with Gaussian grid of 2.8° between 65.58°S and 65.58°N and weighted equal-area grid poleward of 65.58°. There are 26 σ-layers from surface to 2.19 hPa. The physics package was taken from the National Center for Atmospheric Research (NCAR) Community Atmospheric Model, Version 2 (CAM2) (Collins et al. 2003). The sea ice and land component models are respectively the NCAR sea ice model (CSIM4) (Bettge et al. 1996) and the NCAR common land model (CLM2.0) (Bonan et al. 1997). We adjust the land-sea mask and horizontal resolution of land and sea ice models to match those of atmospheric and oceanic models. More details of the model can be found in Yu et al. (2007).

In this study, in order to be consistent with the way cooling and warming are applied in Sun et al. (2004), we stripped the full FGOALS to a simpler version in which daily heat, momentum and fresh water fluxes are exchanged in the tropical Pacific between 10^{o}S-10^{o}N only. Outside of 10^{o}S-10^{o}N of the tropical Pacific, the AGCM and OGCM are not coupled but forced with the observed forcing. The AGCM is forced with the observed

climatological SST and sea ice distribution. The OGCM is forced with the observed climatological wind stress, fresh water flux, and heat flux calculated from a restoring thermal boundary condition in which the restoring SST is the observed climatological SST. We conducted a control run, an extra-tropical cooling run, and an extra-tropical warming run with this coupled GCM. The extratropical cooling and warming imposed over the ocean's surface are the same as in Sun et al. (2004). The length of the run for all three runs is 80 years. We use the last 40 model years in this study.

In order to isolate the effects of the air-sea interaction on the response of the mean tropical Pacific climate to extra-tropical warming and cooling, we carry out three additional experiments with the ocean component model of the aforementioned coupled GCM: a control run, an extra-tropical cooling run, and an extra-tropical warming run. The perturbations are again either extratropical cooling and warming and take the same form as in the coupled experiments. For these three uncoupled experiments with the ocean component, we use climatological surface forcing everywhere including the equatorial region (i.e., the wind stress, the restoring SST, and freshwater flux that have no interannual variations). Thus in these experiments, there are no ENSO events.

Thus, as in Sun et al. (2004), for either extratropical cooling or warming, we have a pair of experiments—one of the experiments is coupled over the equatorial region we call this experiments the case with ENSO or simply the coupled run) and the other experiments is not coupled we call this experiment the case without ENSO or simply the uncoupled run). The coupled runs are 80 years long—the last 40 years were used in the analysis. The forced experiments are 50 years long and the last 10 years were used for the analysis. Note that the purpose here is not compare which run is closer to the observations, but to examine the influence of equatorial ocean-atmosphere coupling on the response of the tropical pacific climate to an imposed extratropical forcing. A summary of the experiments are listed in Table 1.

3 Results

3.1 Control run

Figure 1 shows the climatological annual mean SST (color), precipitation (contour) and wind stress (arrows) of the control run in the tropical Pacific from the tropically coupled GCM (coupling is restricted to the tropical Pacific) and from the full version (globally coupled). The change in the large-scale pattern of SST, wind stress, and precipitation is from the full version to the stripped down version is small. In comparison with observations, there remains a cold bias in the central equatorial Pacific and warm bias in the southeastern Pacific. The cold and warm SST biases are accompanied with an overestimated and underestimated rainfall biases, respectively over these two regions. Consequently, the simulated precipitation appears to be more symmetric about the equator than in the observations, exhibiting the so-called "Double ITCZ" syndrome (Mechoso et al. 1995)—a common bias in the state-of-art coupled models that do not use flux adjustment (Sun et al. 2006). The tropically coupled model has a slightly warmer cold-tongue than the full version. The annual cycle in the stripped-down version is notably more realistic than the full version (Fig. 2). Both versions have pronounced interannual variability. Figure 3 shows the time series of Nino3.4 SST anomaly from the tropically coupled model together with the corresponding time series from the full model. The observed Nino3.4 SST over the last 40 years are also shown for comparison. The amplitude of ENSO in the tropically coupled model is weaker than the full version, but more comparable to the observed. The period of the ENSO in the tropically coupled model is more biannual than the full version. ENSO in both versions is more regular and stronger than in the observations. These differences from observations are common in coupled GCMs (van Oldrenborgh et al. 2005.) The spatial patterns of the SST anomaly associated ENSO from these two versions and the observations are shown in Fig. 4. As in many other coupled models, the anomaly extended too far to the west, but the overall feature resembles the observations well. More detailed discussion about the climatology and variability in this model can be found in (Yu et al. 2007)

3.2 Extratropical cooling experiments

Fig. 5a and 5b show respectively the response of the climatological annual mean SST in

the case without ENSO (equatorial ocean-atmosphere is not coupled) and in the case with ENSO (equatorial ocean-atmosphere is coupled) to the extratropical cooling. In the uncoupled experiment (Fig. 5a), the response of the SST of the equatorial Pacific to the imposed cooling about 1^{o}C over the extratropical Pacific is weak: the cooling is less than 0.2^{o}C and is confined to the eastern Pacific only. When air-sea interaction is considered in the coupled model, however, the cooling to the equatorial surface ocean is enhanced to about 0.4^{o}C, and this cooling extends to the western tropical Pacific (Figure 5b). The corresponding seasonal march of the SST difference between the extra-tropical cooling and control runs from the coupled GCM is further shown in Fig. 6a together with the corresponding seasonal march of the zonal wind stress and the net surface heat flux. The figure shows a reduced seasonal cycle. The strongest cooling is about 0.8^{o}C and occurs in the first half year (Fig. 6a) and this corresponds to a period with enhanced easterly wind stress in the middle and western Pacific (Fig. 6b). The corresponding evolution of the changes in the net surface heat flux shows that it acts as a negative feedback that damps the SST changes (Fig. 6c).

The response of the entire equatorial upper ocean temperature to the imposed extratropical cooling is shown in Fig. 7. The upper panel is for the case without ENSO (uncoupled run) and the bottom one is for the case with ENSO (coupled run). In the case without ENSO, the maximum cooling can be found in the thermocline with maximum value about 0.7^{o}C. As in the experiments of Sun et al. (2004), the cooling is largely confined to the subsurface. The surface cooling is only 0.2^{o}C. Note that the sea surface temperature is restored to the observed SST in the uncoupled model. The cooling to the surface is largely limited to the eastern Pacific, resulting in a weak increase in the zonal SST contrast.

In the coupled run, the response of the equatorial upper ocean temperature has almost completely different pattern: the subsurface cooling is substantially reduced. In fact, the subsurface of the western Pacific even has slightly positive anomaly. The cooling is no longer confined to the subsurface ocean. Instead, it extends to the surface of the entire equatorial ocean. Because in this case, the equatorial zonal wind stress is coupled to the SST gradients, the subsurface temperature is not only affected by the extratropical cooling but also by the zonal wind stress in the coupled run. Because the extratropical

cooling to the equatorial upwelling water through the "ocean tunnel" (Pedlosky 1987, Liu et al 1994, McCreary and Lu 1994) alone results in an increased zonal SST contrast (Fig. 7a), the zonal wind stress is then enhanced. The enhanced zonal wind stress can deepen mean depth as well as the zonal tilt of thermocline (Jin 1996, Sun 1997)—a configuration that favors stronger ENSO events. Figure 8 shows the standard deviation of monthly mean SST from the control and extratropical cooling runs by the coupled GCM. The ENSO amplitude is enhanced in the extratropical cooling run. As shown in Figure 7a, in the absence of coupling, the imposed extratropical cooling increase the temperature contrast between the western Pacific surface water and the thermocline water, and thereby constitutes a destabilized effect of the ocean-atmosphere system. A stronger ENSO is expected to neutralize this destabilization.

The meridional section of temperature changes averaged 90^{o}W-150^{o}W from extratropical cooling run is shown in Figure 9. Although the external forcing is superimposed in the extratropical surface ocean, both coupled and uncoupled runs show a relatively large surface cooling centered at the equator. The weakest surface cooling can be found between 5^{o}-10^{o}N(S). This pattern of cooling is consistent with the "ocean tunnel" effect: colder water penetrates into equatorial thermocline through subduction along isentropic surfaces (Pedlosky 1987, Liu et al 1994, McCreary and Lu 1994). Consequently, the surface water off the equator between 5^{o}-10^{o}N(S) is hardly affected by the extratropical cooling. Having compared temperature changes from the uncoupled run with those from coupled run, two distinctive things can be found. The first one is that the subsurface cooling along the equator is weakened in the coupled run as shown in Figure 7. This is due to stronger vertical water exchange in the coupled run induced by air-sea interaction. On the other hand, the amplitude of cooling in the extratropical region in both the surface and subsurface is also reduced in the coupled run. Because the air-sea interaction is turned off in the extratropical region and the same external forcing is applied in coupled and uncoupled runs, the weakened extratropical cooling in the coupled run results from an enhanced poleward heat transport by oceanic circulation.

3.3 Extratropical warming experiments:

Extratropical warming experiments generally show reversed patterns as the extratropical

cooling ones. Fig. 10 shows the SST changes in response to an imposed extratropical warming. The upper panel is for the case without ENSO (uncoupled run) and the lower panel is for the case with ENSO (coupled run). In the case with ENSO, the extratropical warming leads to about 0.2 ^{o}C warming in the eastern equatorial Pacific (Fig.10 b). In the case with ENSO, the tropical warming is strengthened to 0.4 ^{o}C and the warming extends all the way to the western Pacific.

Figure 11 shows equatorial temperature changes from extratropical warming experiments in the case without ENSO and the case with ENSO. Fig. 11a is for the case without ENSO, and Fig.11b is for the case with ENSO. Fig.11a and Fig. 11b are about the reverses of Fig. 7a and Fig.7b. In the absence of coupling, the effect of the imposed extratropical warming on the equatorial upper ocean temperature is largely confined to the thermocline. In the present of coupling, the response of the upper ocean temperature resembles an El Nino pattern. The eastern Pacific is much warmer while the subsurface of the western Pacific actually gets cooler.

Closer comparison between the warming case and the cooling case reveals differences that may be of significance. The imposed cooling and the heating over the extratropical Pacific is the same, but Fig.7a and Fig.11a show that the equatorial thermocline temperature response to the cooling more sensitively (0.7^{o}C cooling versus 0.5^{o}C warming). There are no noticeable asymmetries in the coupled experiments, though. In response to the weakened zonal SST gradients, the zonal winds become weaker, which result in a flattening and shoaling of the thermocline. Compared with the control run of coupled model, the extratropical warming run reveals pronounced subsurface warming along the thermocline, consequently resulting in a weakened temperature contrast between surface temperature in the western Pacific and that in the thermocline. This change implies a stabilized effect of the ocean-atmosphere system. Indeed, ENSO in the case with warming imposed is weaker (Fig. 12).

The pattern of meridional section of temperature changes from extratropical warming is quite similar to the case of extratropical cooling but there are some differences (Figure 13). For example, a uniform cooling can be found along the equator in the extratropical

cooling case without ENSO, but in the corresponding extratropical warming case, the warming can only be found above 200m. Below this depth in the extratropical warming case, the response is actually cooling. In the coupled case (i.e, the case with ENSO), coupled extratropical cooling run shows weakened extratropical cooling in the both hemispheres, and the coupled extratropical warming run shows weakened extratropical warming in the Southern Hemisphere only.

4. Summary

Following the study of Sun et al. (2004), we have conducted an extended investigation of the role of equatorial ocean-atmosphere coupling in extratropcial and tropical interactions—particularly how the equatorial coupling affects the response of the tropical Pacific upper ocean to extratropical cooling/warming. The extratropical warming and cooling experiments are carried out with a regionally coupled GCM—ocean—atmosphere is only coupled over the equatorial Pacific. Experiments were conducted in pairs. In one of the experiments, ocean-atmosphere over the equatorial region is switched off, and therefore ENSO is not present. When the equatorial ocean-atmosphere is not coupled no ENSO), extratropical cooling/warming respectively increases and decreases the thermal contrast between the warmpool SST (Tw) and the characteristic temperature of the equatorial thermocline water (Tc) (i.e., respectively destabilizes and stabilizes the coupled equatorial ocean-atmosphere system). Comparing coupled experiments with and the uncoupled experiments, it can be found that the equatorial air-sea interaction or the presence of ENSO) reduces the response of Tw-Tc through stronger vertical exchange of heat induced by ENSO in the coupled run. ENSO amplitude is enhanced in the extratropical cooling run and reduced in the extratropical warming run. The response of ENSO amplitude to the cooling in the present model appears to be less sensitive as in the model of Sun et al. (2004), possibly because the control run in the present model already has very strong ENSO. The response of ENSO frequency to extra-tropical cooling/heating is also compared, but we have not found any significant change in period. Also, by contrasting the extratropical warming runs with the corresponding cooling runs, we find that the mean tropical climate is more sensitive to

extratropical cooling than to extratropical warming, particularly in the case in the absence of coupling, suggesting a potential role of the buoyancy effects.

To be in line with Sun et al. (2004), and taking a step-by-step approach, we have limited ocean-atmosphere coupling in the coupled experiments to the equatorial Pacific. We plan to carry out additional perturbation experiments in which ocean-atmosphere over extratropical Pacific are also allowed to couple. These experiments are more technically difficult but will allows us to investigate whether the role of ENSO as delineated in Sun et al. (2004) and in the present study in facilitating the remote forcing from the extratropcial ocean onto the equatorial ocean still holds in a more realistic setting. As in other models, the present model has a cold bias. We will need to investigate whether and how the tropical cold bias may impact the response of the coupled model to extratropical cooling or warming.

Tropical-extratropical interaction though the "Ocean Tunnel" (Pedlosky 1987, Liu et al. 1994, McCreary and Lu, 1994) has been hypothesized as an important mechanism for decadal variability in the Pacific (Deser et al. 1996, Gu and Philander 1997). The role of ENSO—or more generally the equatorial ocean-atmosphere coupling—has not been adequately considered in these studies. By delineating the role of equatorial ocean-atmosphere coupling in the tropical-extratropical interaction, the present study may also help to advance our understanding of the decadal variability in the tropical Pacific. In the same vein, the present study may also help to understand the Pacific climate change over centennial and longer time-scales. For example, Cobb et al. (2003) has found that during the little ice age—a period during which significant cooling was registered in extratropical regions (Bradley et al. 2003), ENSO was more energetic than many other periods during the last millennium. Conversely, the proxy data by Rein et al. (2004) suggests a weak ENSO activity during the medieval warm period—a period during which significant warming was observed in the extratropical regions. The present study may help to understand these paleoclimate observations.

Because the climate response in the tropical Pacific to increased greenhouse gases has been paid to more and more attention, the present study may also help to understand the

response of the tropical Pacific climate to global warming. So far, most of the efforts in understanding the response of the tropical Pacific climate to global warming simulated by coupled GCMS have largely been concentrated on factors within the tropics (Knutson and Manabe 1995, Meehl and Washington 1996, Vecchi et al. 2006, DiNezio et al. 2009). The present study suggests that a tropical perspective alone may not be adequate in understanding the effects of global warming on the level of ENSO activity or on the mean state, particularly in consideration that the changes in the mean tropical upper ocean stratification already includes the response of ENSO to extratropical forcing.

ACKNOWLEGEMENT

The study is jointly supported by a grant from the National Basic Research Program of China (2007CB411806) and NSFC grants (No.40675049, and No. 40821092). .-Z. Sun was partially supported by US NSF's Climate and Large-Scale Dynamics Program and US NSF's Physical Oceanography Program (ATM-9912434, ATM—0331760, and ATM 0553111). We are grateful to the editor Dr. Shangping Xie, and to the two anonymous reviewers, for their comments and suggestions.

References

Bettge,T.W., J.W. Weatherly, W.M. Washington, D. Pollard, B.P. Briegleb, and W. G. Strand, Jr., 1996: "The CSM Sea Ice Model." NCAR Technical Note NCAR/TN-425+STR, National Center for Atmospheric Research, Boulder, Colorado.

Bonan, G. B., K. W. Oleson, M. Vertenstein, S. Levis, X. Zeng, Y., Dai, R. E. Dickson, and Z.-L. Yang, 2002: The land surface climatology of the Community Land Model coupled to the NCAR Community Climate Model. J. Climate, 15, 3123−3149.

Bradley R.S., M.K. Hughes, H. F. Diaz, 2003: Climate in Medieval Time. *Science,* **302**, 404-405.

Bush, A. B. G., and S. G. H. Philander, 1998: The role of ocean-atmosphere interactions in tropical cooling during the Last Glacial Maximum. *Science***, 279,** 1341-1344.

Cobb, K.M., C.D. Charles, H. Cheng, and R. L. Edwards, 2003: El Nino/Southern Oscillation and tropical Pacific climate during the last millennium. *Nature*, **424,** 271-276.

Collins, W. D., J. J. Hack, B.A. Boville, P. J. Rasch, D. L. Williamson, J. T. Kiehl, B. Briegleb, J. Mccaa, C. Bitz, S.-J. Lin, R. B. Rood, M.-H. Zhang, and Y.-J. Dai, 2003: Description of the NCAR Community Atmosphere Model (CAM2), NCAR Technical Notes, 189 pp., NCAR, Boulder, Colo., USA. (http://www.ccsm.ucar.edu/models/atm-cam/docs/cam2.0/description/index.html)

Deser,C., M.A. Alexander, M.S. Timlin, 1996: Upper ocean thermal variations in the North Pacific during 1970-1991. *J. Climate,* **9**, 1840-1855.

DiNezio, P. N., A. C. Clement, G. A. Vecchi, B. J. Soden, Benjamin P. Kirtman, and

Sang-Ki Lee, 2009: Climate Response of the Equatorial Pacific to Global Warming. *J. Climate* (In press)

Federov, A, P S Dekens, M McCarthy, A C Ravelo, P B deMenocal, M Barreiro, Ronald C Pacanowski, and S.G.H. Philander, 2006: The Pliocene Paradox (Mechanisms for a Permanent El Niño). 312(5779), 1485-1489.

Gu, D., and S. G. H. Philander, 1997: Interdecadal Climate Fluctuations That Depend on Exchanges Between the Tropics and Extratropics. Science, 275(5301), 805-807, DOI: 10.1126/science.275.5301.805

Jin, F.-F., 1996: Tropical ocean-atmosphere interaction, the Pacific cold tongue, and the El Niño-Southern oscillation. *Science,* **274,** 76-78.

Liu, H.L., Zhang, X.H., Li, W., Yu, Y.Q. and Yu R.C., 2004: An eddy-permitting oceanic general circulation model and its preliminary evaluations, Adv. Atmos. Sci., Vol. 21, 675-690.

Liu, Z., S.G.H. Philander, and P.C. Pacanowski, 1994: A GCM study of tropical-subtropical upper-ocean water exchange. *J. Phys. Oceanogr.* **24**, 2606-2623.

Liu, Z., S. J. Vavrus, F. He, N. Wen, and Y. Zhang, 2005: Rethinking tropical ocean response to global warming: The enhanced equatorial warming. *J. Climate.*, **18**, 4684–4700.

Knutson, T. R., and S. Manabe, 1995: Time-mean response over the tropical Pacific to increased CO2 in a coupled ocean-atmosphere model. *J. Climate,* **8**, 2181–2199.

McCreary, J.P., and P. Lu, 1994: On the interaction between the subtropical and the equatorial oceans: The Subtropical Cell. *J. Phys. Oceanogr*., **24**, 466-497.

Mechoso, C. R., and Coauthors, 1995: The Seasonal cycle over the tropical Paci¯c in coupled ocean-atmosphere general circulation models. Mon. Wea. Rev., 123,

2825-2838.

Meehl, G. A., and W. M. Washington, 1996: El Niño-like climate change in a model with increased atmospheric CO2 concentrations. *Nature*, **382**, 56–60.

Neelin, J. D., D. S. Battisti, A. C. Hirst, F.-F. Jin, Y. Wakata, T. Yamagata, and S. Zebiak, 1998: ENSO theory. J. Geophys. Res.,103, 14 261–14 290.

Pedlosky, J., 1987: An inertial theory of the equatorial undercurrent. *J.Phys. Oceanogr*., **17**, 1978- 1985.

Rein, Bert (2005), El Niño variability off Peru during the last 20,000 years, Paleoceanogr, 20, PA4003, doi:10.1029/2004PA001099.

Rodgers, K. B., P. Friederichs, and M. Latif, 2004: Tropical Pacific decadal variability and its relation to decadal modulations of ENSO. *J. Climate,* **17,** 3761–3774.

Schopf, P. and R. Burgman, 2006: A Simple Mechanism for ENSO Residuals and Asymmetry. *J. Climate*, **19**, 3167-3169.

Sun, D.-Z., 2000: Global climate change and ENSO: A theoretical framework. El Nin˜o: Historical and Paleoclimatic Aspects of theSouthern Oscillation, Multiscale Variability and Global and Regional Impacts, H. F. Diaz and V. Markgraf, Eds., Cambridge University Press, 443–463.

Sun, D.-Z., 2003: A possible effect of an increase in the warm-pool SST on the magnitude of El Nin˜o warming. J. Climate, 16, 185–205.

Sun, D.-Z., 2004: The Control of Meridional Differential Heating Over the Level of ENSO activity: A Heat-Pump Hypothesis. page 71-83. In Earth's Climate: The Ocean-Atmosphere Interaction, AGU Geophysical Monograph, Vol. 147, 414 pages. Edited by C. Wang, S.-P. Xie, and J. Carton.

Sun, D.-Z., 1997: El Niño: a coupled response to radiative heating? Geophys. Res. Lett., 24, 2031-2034.

Sun, D.-Z. and T. Zhang 2006: A Regulatory Effect of ENSO on the Time-Mean Thermal Stratification of the Equatorial Upper Ocean. Geophys. Res. Lett., Vol. 33, L07710, doi:10.1029/2005GL025296

Sun, D.-Z., T. Zhang, and S.-I. Shin, 2004 : The effect of subtropical cooling on the amplitude of ENSO: a numerical study. J. Climate , 17, 3786-3798.

Sun, F.. and J.-Y.-Yu, 2008: A 10-15 year Modulation Cycle of ENSO Intensity, J. Climate, Accepted.

Trenberth, K. E., G. W. Branstator, D. Karoly, A. Kumar, N.-C. Lau, and C. Ropelewski, 1998: Progress during TOGA in understanding and modeling global teleconnections associated with tropical sea surface temperatures. J. Geophys. Res., 103, 14 291–14 324.

Van Oldenborgh, G.J. van, S.Y. Philip and M. Collins, El Niño in a changing climate: a multi-model study. Ocean Science, 2005, 1, 81-95, sref:1812-0792/os/2005-1-81.

Vecchi, G. A., B. J. Soden, A. T. Wittenberg, I. M. Held, A. Leetmaa, and M. J. Harrison, 2006: Weakening of tropical Pacific atmospheric circulation due to anthropogenic forcing. *Nature*. **441**, doi:10.1038/nature04744.

Wang, B., Wan, H., Ji, Z.Z., Zhang, X.H., Yu, R.C., Yu, Y.Q. and Liu, H.L., 2004: Design of a new dynamical core for global atmospheric models based on some efficient numerical methods, Science in China, Ser. A, Vol. 47 Supp., 4-21.

Wang, C., and J. Picaut, 2004: Understanding ENSO physics - A review. In: Earth's Climate: The Ocean-Atmosphere Interaction. C. Wang, S.-P. Xie, and J. A. Carton, Eds., AGU Geophysical Monograph Series, 147:21-48.

Xiao Chan, Yu Yongqiang, 2006: Shape-Preserving Advection Scheme and its Application in an OGCM. Progress in Natural Sciences 16 1442−1448. In Chinese)

Yu, Y., H. Zhi, B. Wang, H. Wan, C. Li, H. Liu, W. Li, W. Zheng, T. Zhou, 2008: Coupled Model Simulations of Climate Changes in the 20th Century and Beyond. Adv. Atmos. Sci., 25,641-654.

Zhang, X., et al., 2003:The development and application of the Oceanic General Circulation Models Part I. The Global Oceanic General Circulation Models. Chinese J. of Atmos. Sci., 27, 607-617. (In Chinese)

Table Legends:

Table 1: A summary of the experiments.

Table 1 Experiments

Experiment	Coupling	Extra-tropical Conditions	ENSO?
A	10°S-10°N	Climatology	Yes
B	10°S-10°N	Warming	Yes
C	10°S-10°N	Cooling	Yes
D	None	Climatology	No
E	None	Warming	No
F	None	Cooling	No

Table 1: A Summary of the experiments.

Figure Legends

Figure 1 Climatologica annuall mean SST (shaded), precipitation (contour), and wind stress (vector) in the tropical Pacific from the control run by the tropically coupled GCM (a) and the globally coupled GCM (Unit: ^{o}C) Data from the 41st to 80th model year were used for this plot).

Figure 2: The seasonal cycle of the SST (averaged over 2^{o}S-2^{o}N) for the two versions of the model—tropically coupled only version and the globally coupled version-- (a, b) and the observations.

Figure 3 Monthly mean Nino3.4 index from the control run of the tropically coupled GCM (red) and the full version (black) and observation (green). (Unit : ^{o}C)

Figure 4. Spatial pattern of SST anomaly associated with ENSO as represented by the leading EOF of the tropical Pacific SST variability within the region 10^{o}S-10^{o}N for the control run of the two versions of the model (a and b), and for the observations (c). Recall that the coupling is restricted to the equatorial region (10^{o}S-10^{o}N).

Figure 5 (a) SST differences between the uncoupled extra-tropical cooling run an the control run. (b) SST differences between the coupled extra-tropical cooling run and the control run (unit : C). The corresponding differences in the surface wind stress are shown as arrows (unit: N/m*m). For the coupled run, the 41st to 80th model year were used in the calculation. For the uncoupled run, the last 10 years of a 50 year long forced run was used.

Figure 6. The seasonal march of the SST differences between the coupled extra-tropical cooling run and the control run (a). (b) and (c) are the corresponding seasonal march of the zonal wind stress differences and the net surface heat flux differences.

Figure 7. Depth-longitude section of temperature difference in ^{o}C) along the equator between the extra-tropical cooling run without ENSO and the control run (a) and between the extratropical cooling run with ENSO and the control run (b). The red line indicates the position the 20C isotherm in the control run. The data used are the same as for Fig. 5.

Figure 8. Standard deviation of monthly mean sea surface temperature for control run (a), extratropical cooling run (b), and the difference between the two runs (c) (unit: ^{o}C). Note that both run are coupled runs. . The data used are the same as for Fig. 5.

Figure 9. Depth-latitude section of temperature difference in ^{o}C) between extra-tropical cooling run without ENSO and the control run (a) and between the extra-tropical cooling run with ENSO and the control run (b). The data used are the same as for Fig. 5.

Figure 10. (a) SST differences between the uncoupled extra-tropical warming run an the control run.(b) SST differences between the coupled extra-tropical warming run and the control run (unit : ^{o}C). The corresponding differences in the surface wind stress are shown as arrows (unit: N/m*m). For the coupled run, the 41st to 80th model year were used in the calculation. For the uncoupled run, the last 10 years of a 50 year long forced run was used.

Figure 11. Depth-longitude section of temperature difference in ^{o}C) along the equator between the extra-tropical warming run without coupling and the control run (a) and between the extratropical warming run with coupling and the control run (b). The data used are the same as for Fig. 10.

Figure 12. Standard deviation of monthly mean sea surface temperature for control run (a), extratropical warming run (b), and the differences between the two runs (c) (unit: C).). The data used are the same as for Fig. 10.

Figure 13. Depth-latitude section of temperature difference in ^{o}C) between extra-tropical warming run without ENSO and the control run (a) and between the extra-tropical warming run with ENSO and the control run (b). The data used are the same as for Fig. 10.

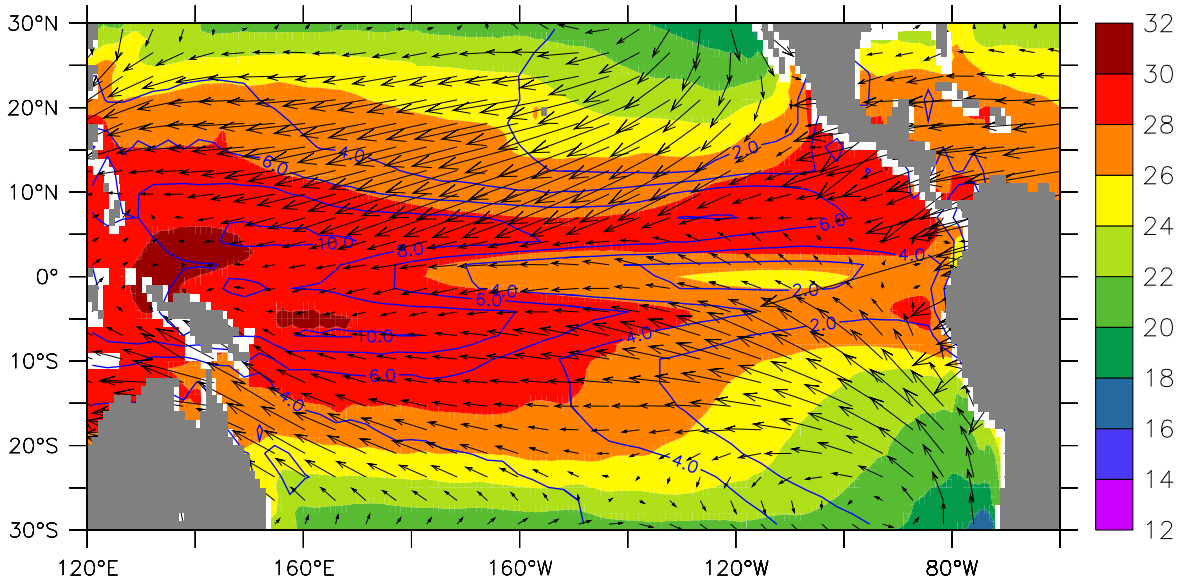

(a)

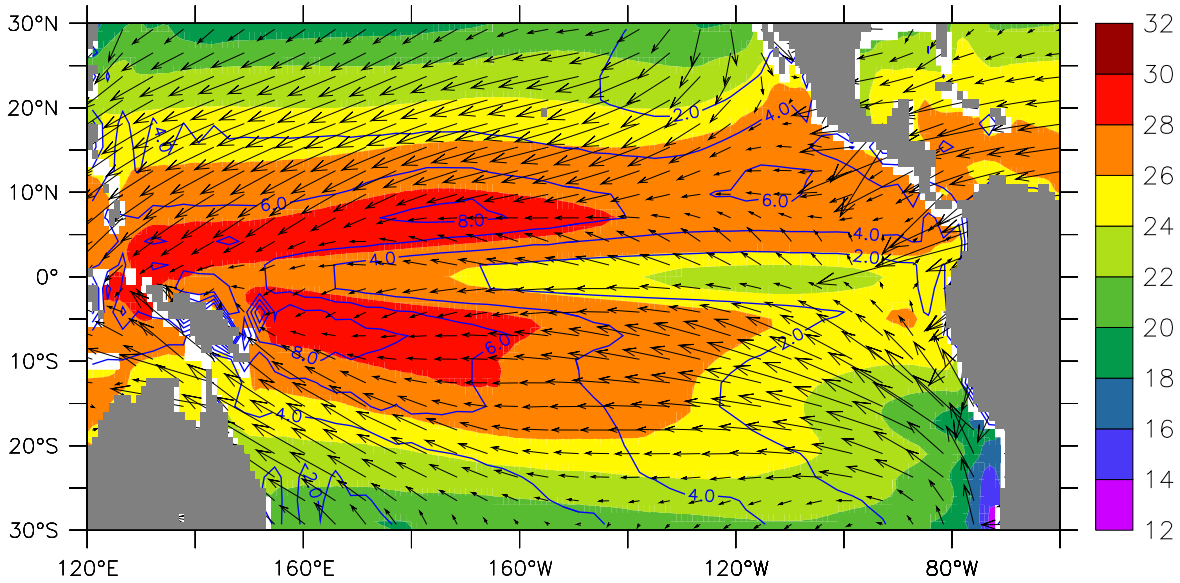

(b)

Figure 1 Climatological mean SST (shaded, unit: C), wind stress (vector, unit : N/(m*m)) and precipitation rate (contour, unit: mm/day) in the tropical Pacific from the control run the tropically coupled GCM(a) and the globally coupled GCM(b), where SSTs from the 41st to 80th model year were used for this plot.

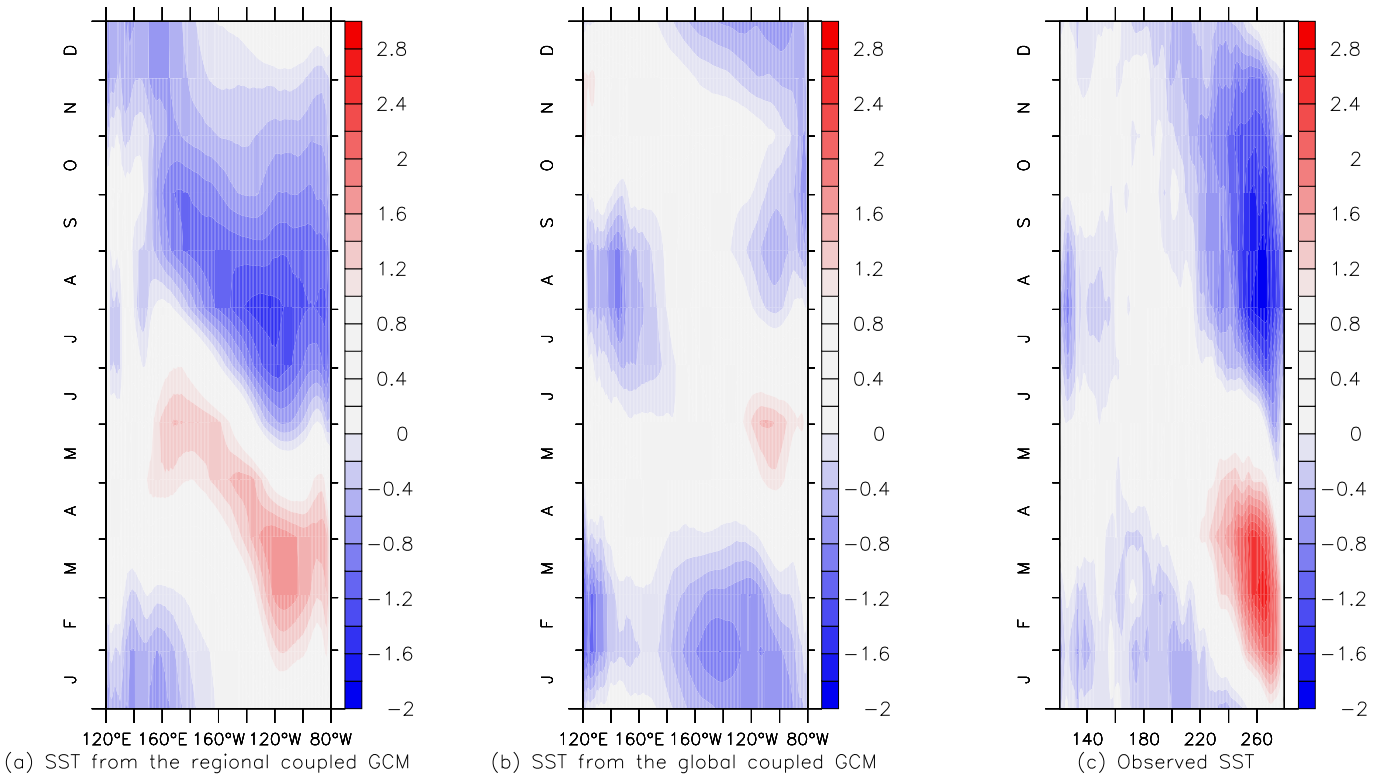

(a) SST from the regional coupled GCM (b) SST from the global coupled GCM (c) Observed SST

Figure 2: The seasonal cycle of the SST (averaged over 2S−2N) for the two versions of the modeltropically coupled only version and the globally coupled version−− (a, b) and the observations (c).

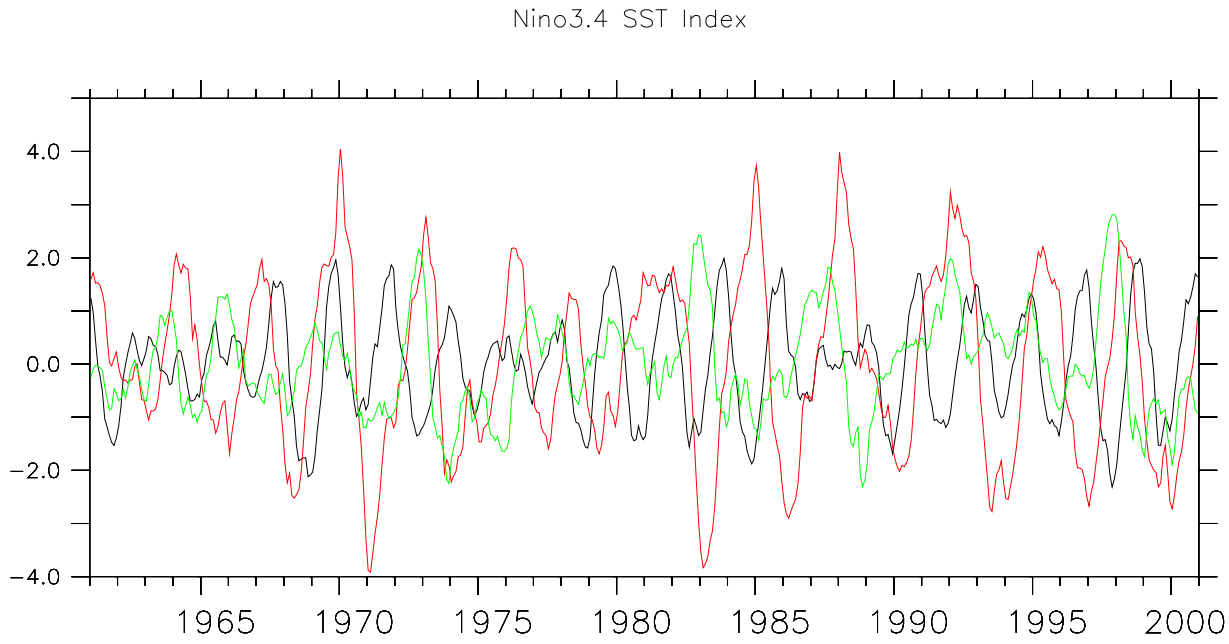

Figure 3 Monthly mean Nino3.4 index from control run by the tropically coupled GCM (red), the full version (black) and observation (green). (unit : C)

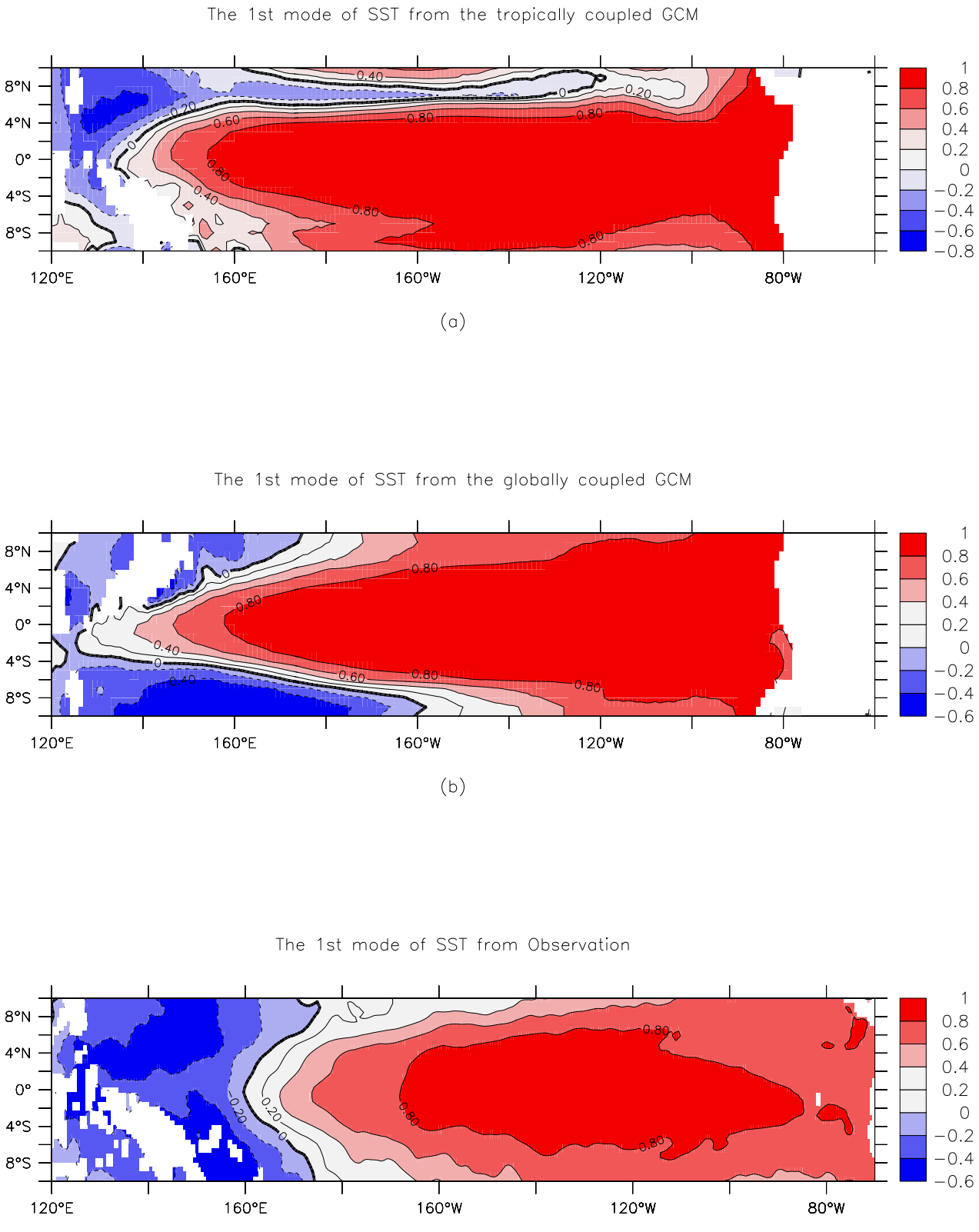

Figure 4 Spatial pattern of SST anomaly associated with ENSO as represented by the leading EOF for the control run of the two versions of the model (a and b), and for the observations (c).

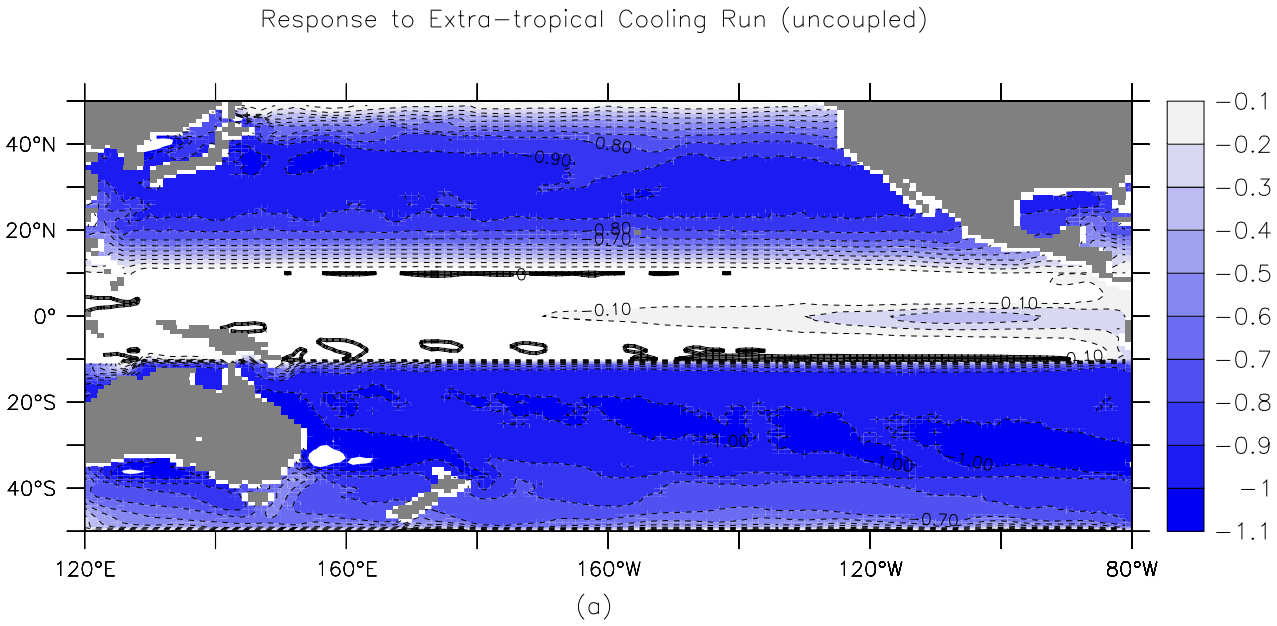

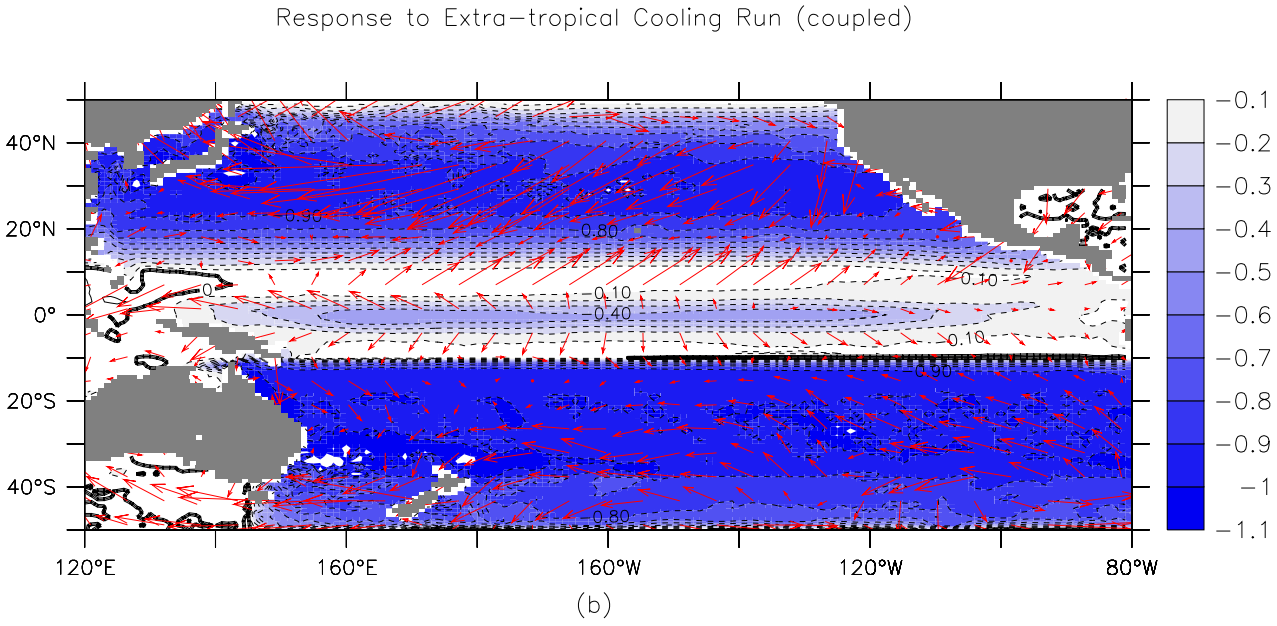

Figure 5 (a) SST differences between the uncoupled extra−tropical cooling run an the control run. (b) SST differences between the coupled extra−tropical cooling run and the control run (unit : C). The corresponding differences in the surface wind stress are shown as arrows (unit: N/mm). For the coupled run, the 41st to 80th model year were used in the calculation. For the uncoupled run, the last 10 years of a 50 year long forced run was used.

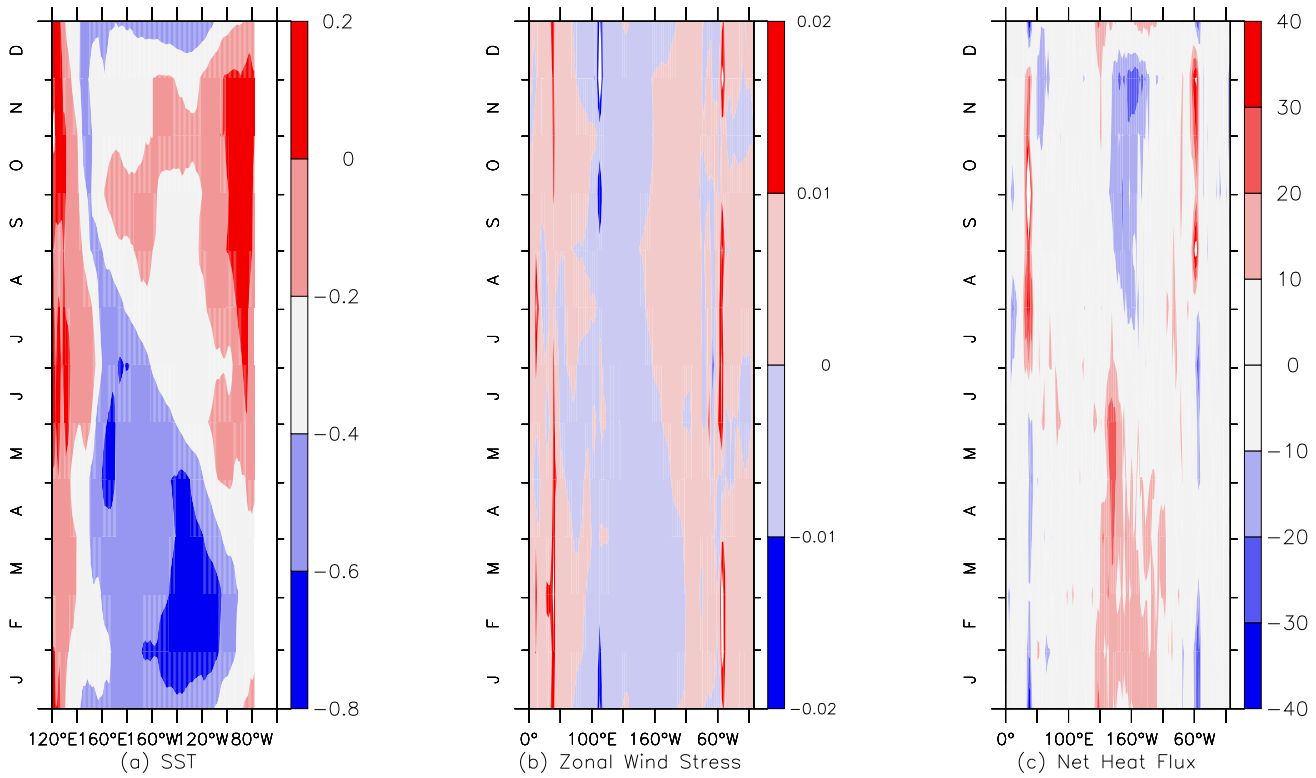

Figure 6. The seasonal march of the SST differences between the coupled extra-tropical cooling run an the control run (a). (b) and (c) are the corresponding seasonal march of the zonal wind stress differences and the net surface heat flux differences.

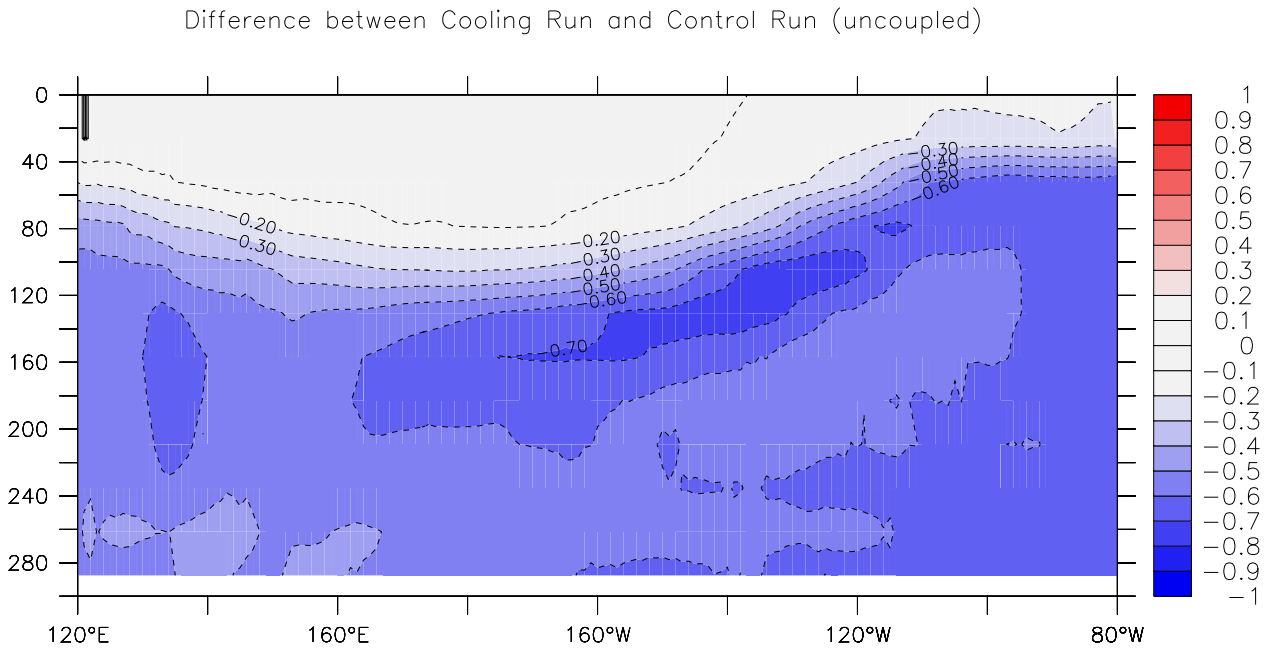

(a)

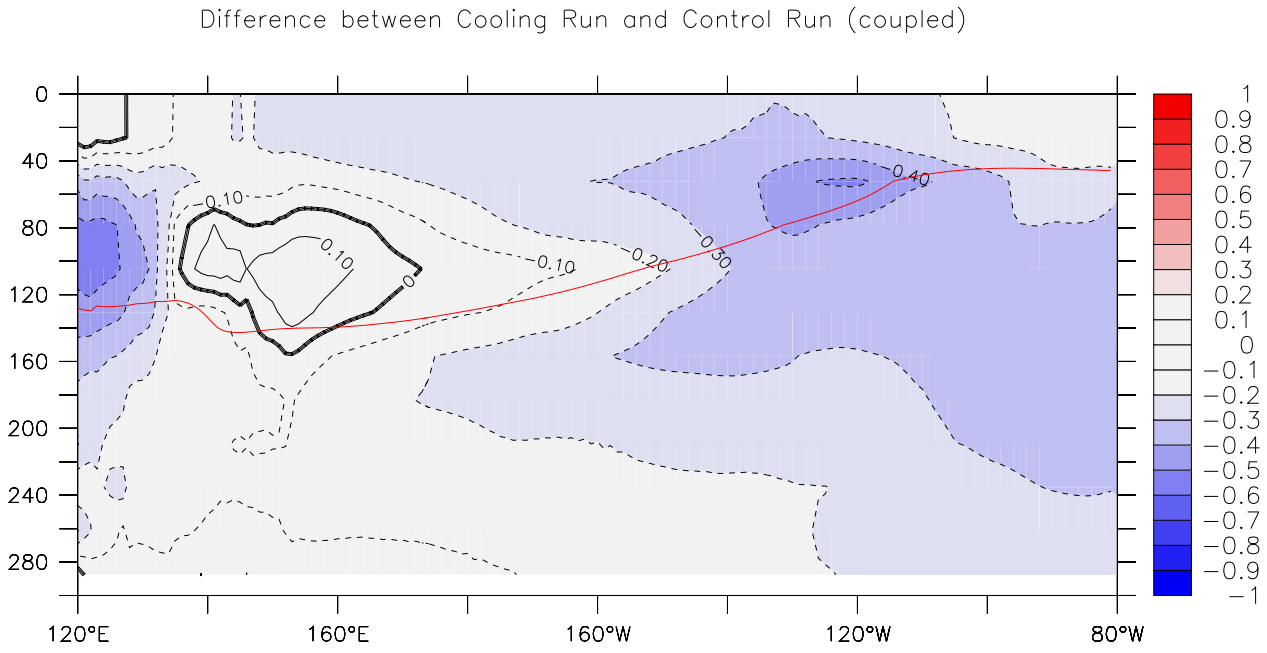

(b)

Figure 7 Depth–longitude section of temperature difference (in C) along the eauator between the extra–tropical cooling run without ENSO and the control run(a) and between the extratropical cooling run with ENSO and the control run (b). The red line indicates the position the 20C isotherm in the control run. The data used are the same as for Fig. 3.

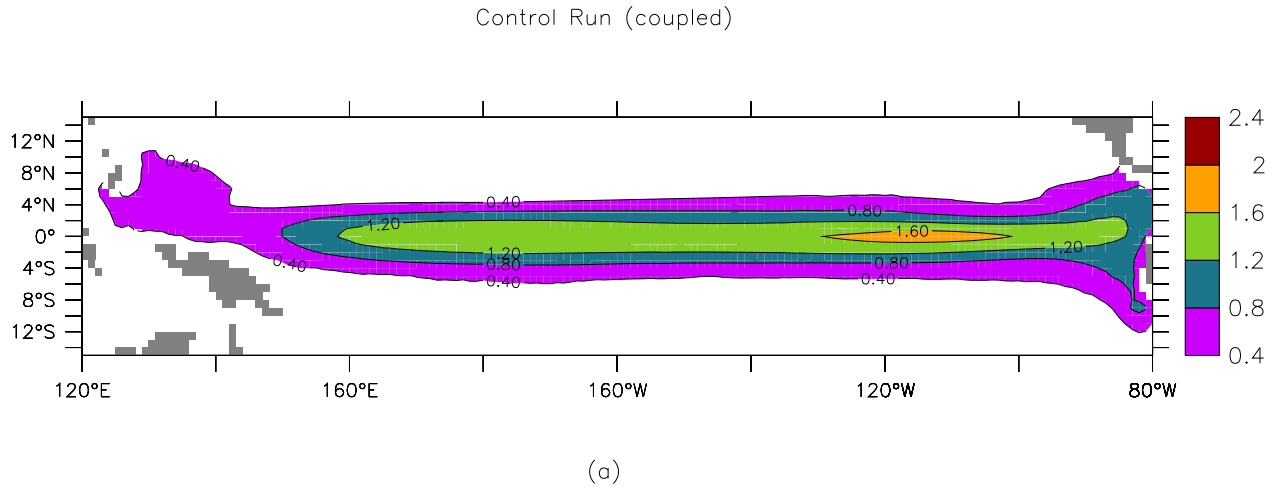

(a)

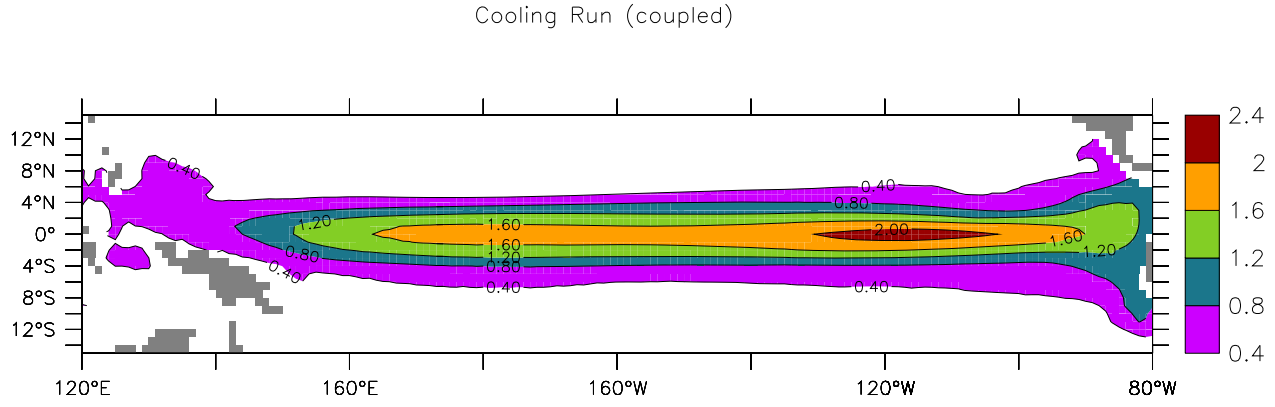

(b)

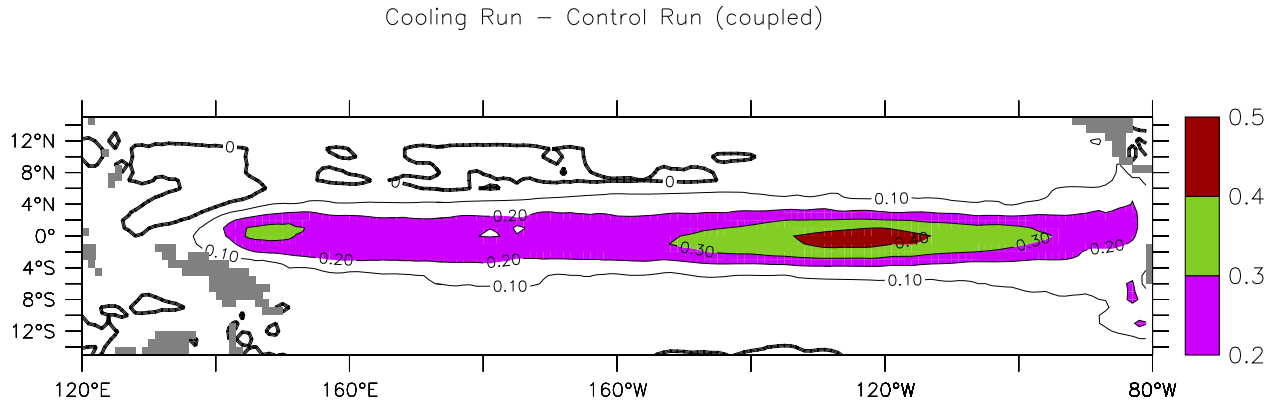

(c)

Figure 8 Standard deviation of monthly mean sea surface temperature for control run (a), extratropical cooling run (b), and (c) difference between extratropical cooling and control runs. (Unit: C) Note that both runs are coupled runs.

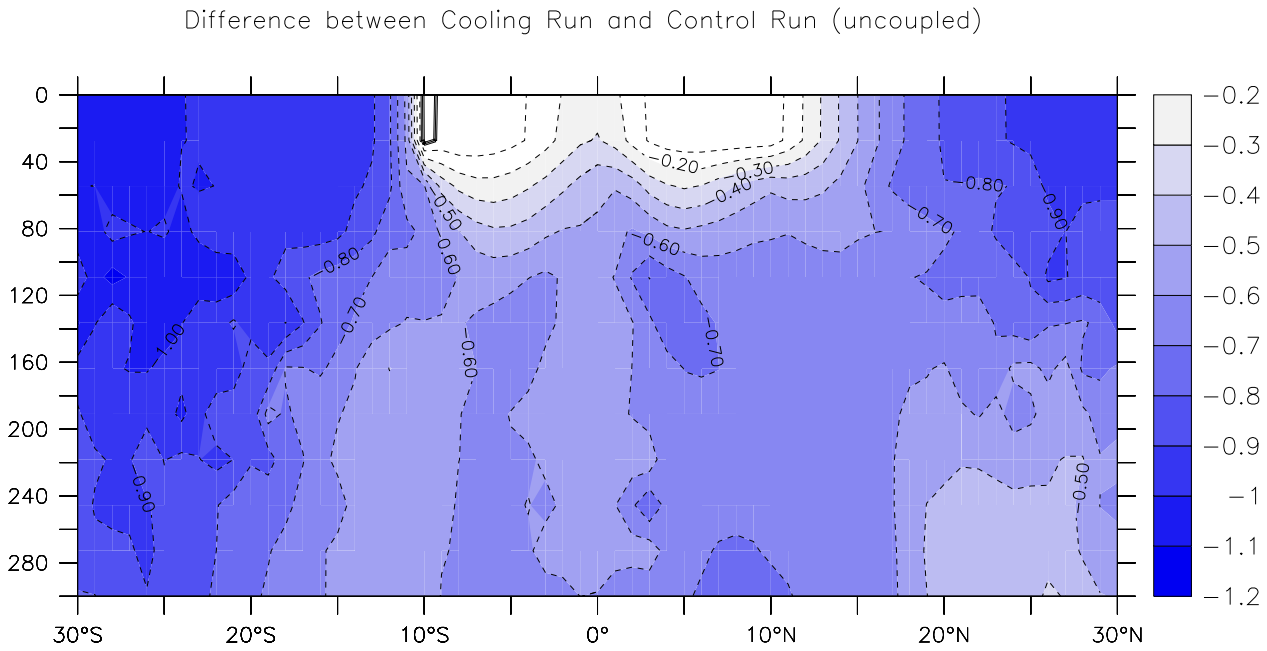

(a)

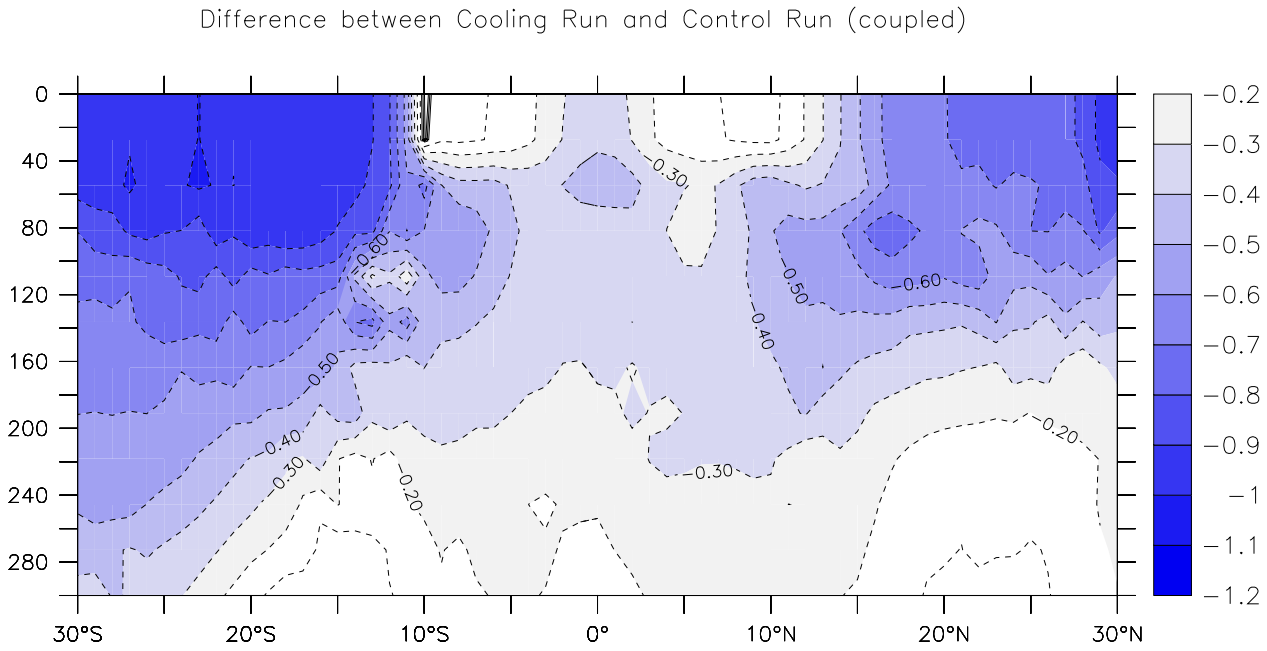

(b)

Figure 9 Depth–latitude section of temperature difference averaged from 90W to 150W (in C) between extra–tropical cooling run and the control run without ENSO (a) and between the extra–tropical cooling run and the control run with ENSO (b). The data used are the same as for Fig. 3.

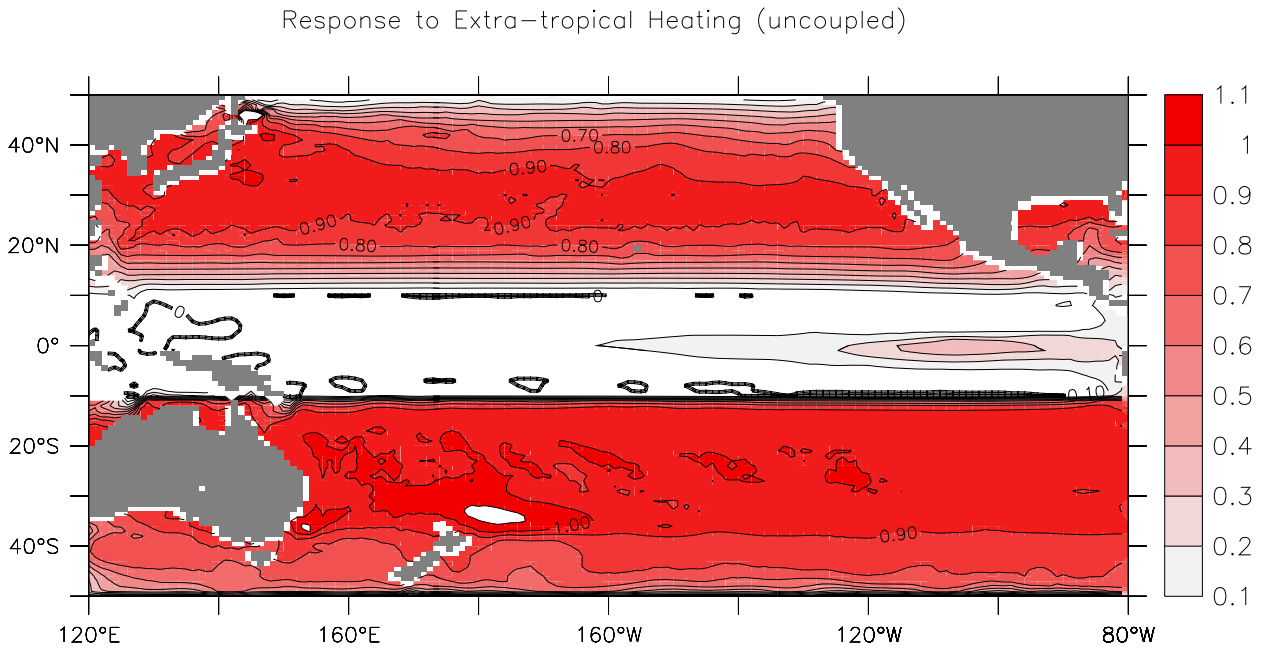

(a)

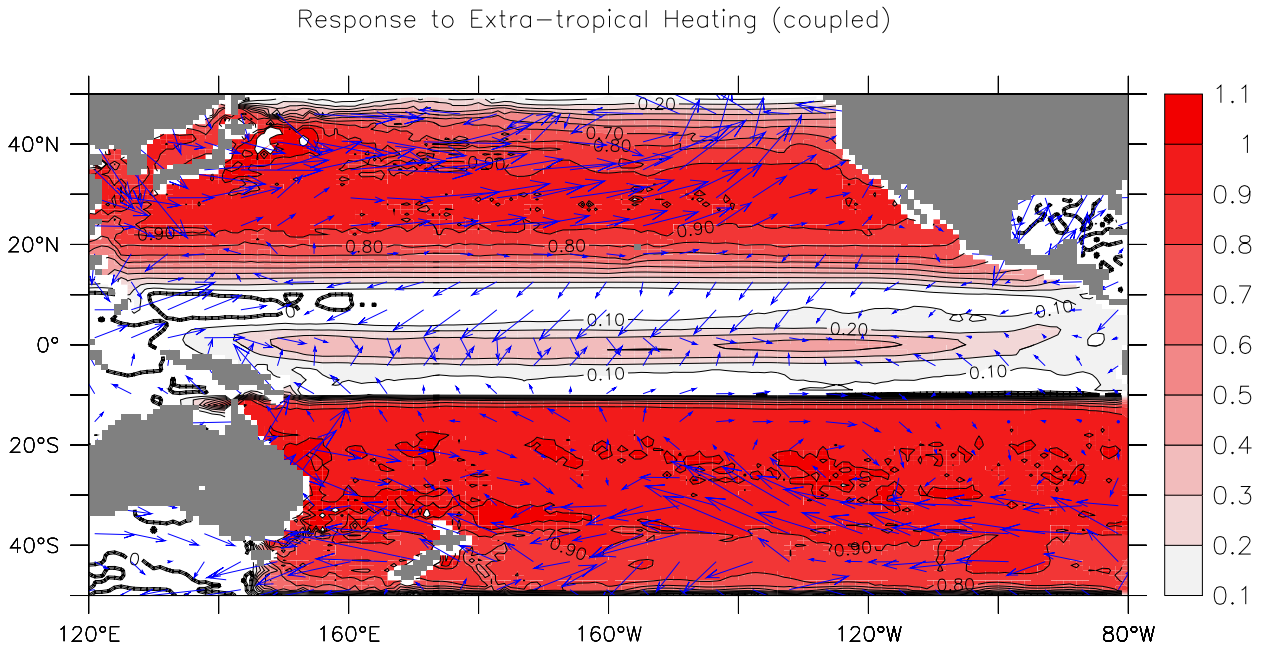

(b)

Figure 10 (a) SST differences between the uncoupled extra−tropical warming run an the control run. (b) SST differences between the coupled extra−tropical warming run and the control run (unit : C). The corresponding differences in the surface wind stress are shown as arrows (unit: N/mm). For the coupled run, the 41st to 80th model year were used in the calculation. For the uncoupled run, the last 10 years of a 50 year long forced run was used.

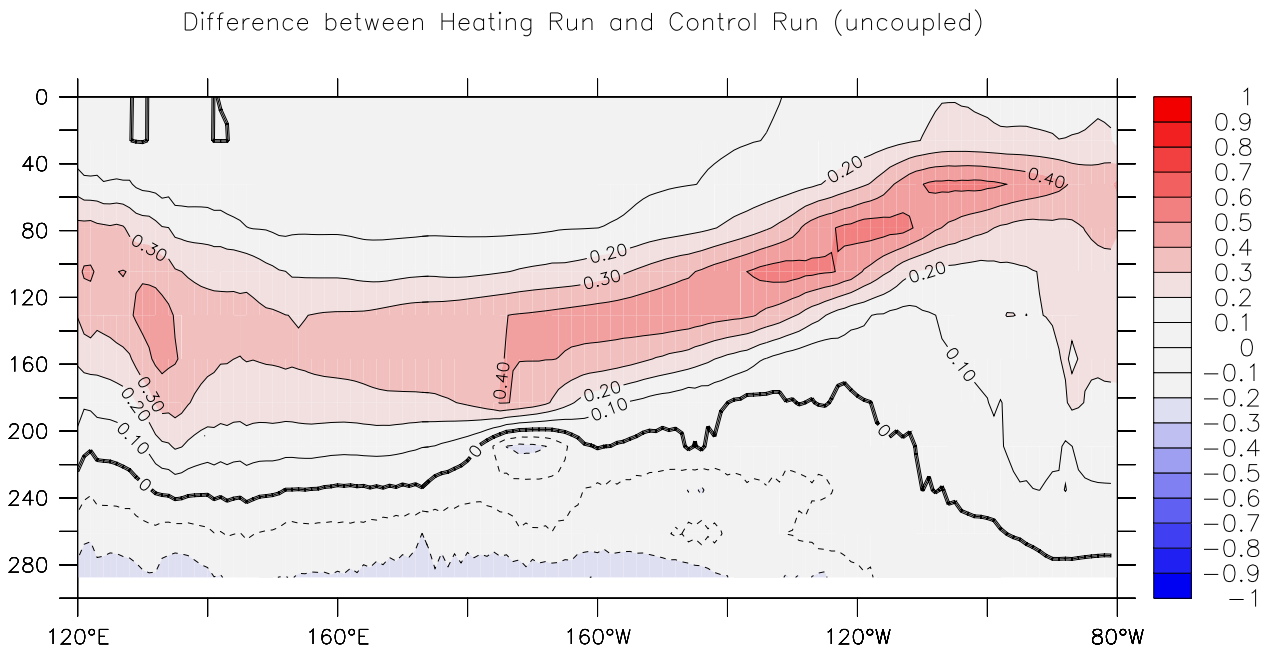

(a)

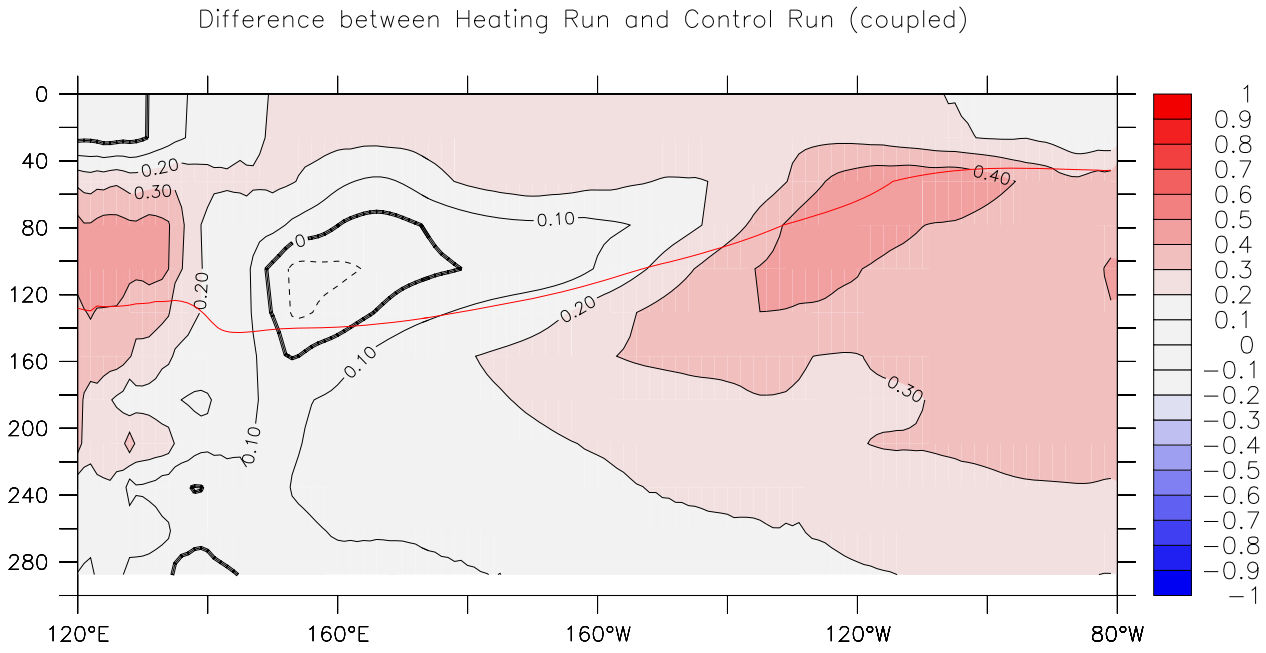

(b)

Figure 11 Depth–longitude section of temperature difference (in C) along the equator between the extra–tropical heating run without ENSO and the control run (a) and between the extratropical heating run with ENSO and the control run (b). The red line indicates the position of the 20C isotherm in the control run. The data used are the same as for Fig. 7.

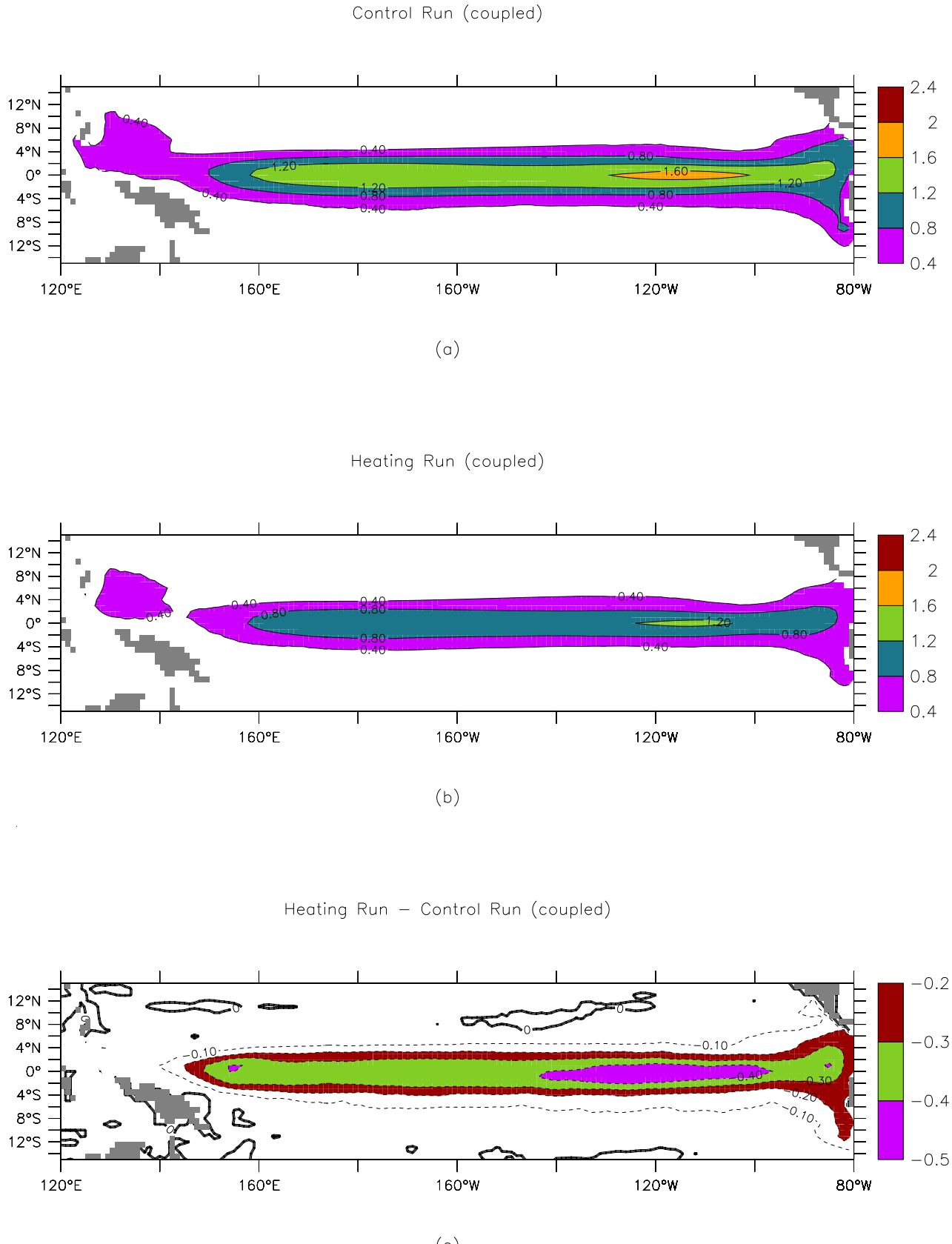

Figure 12 Standard deviation of monthly mean sea surface temperature for control run (a), extratropical heating run (b), and (c) difference between extratropical heating and control runs. (Unit: C)

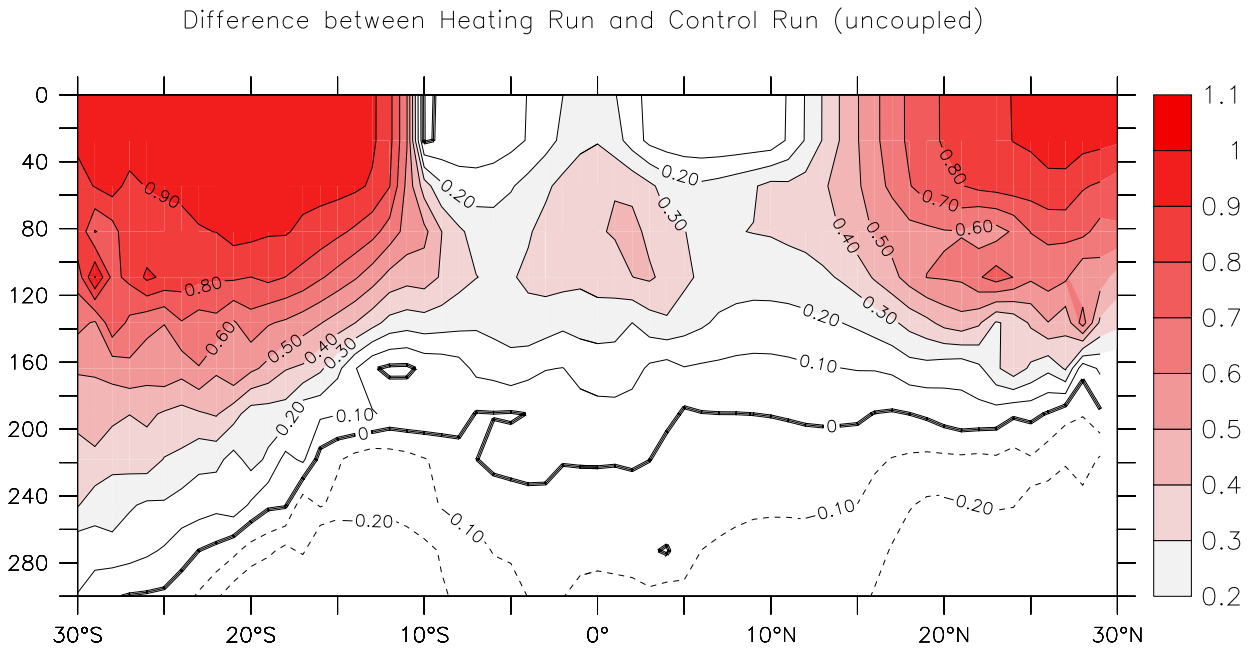

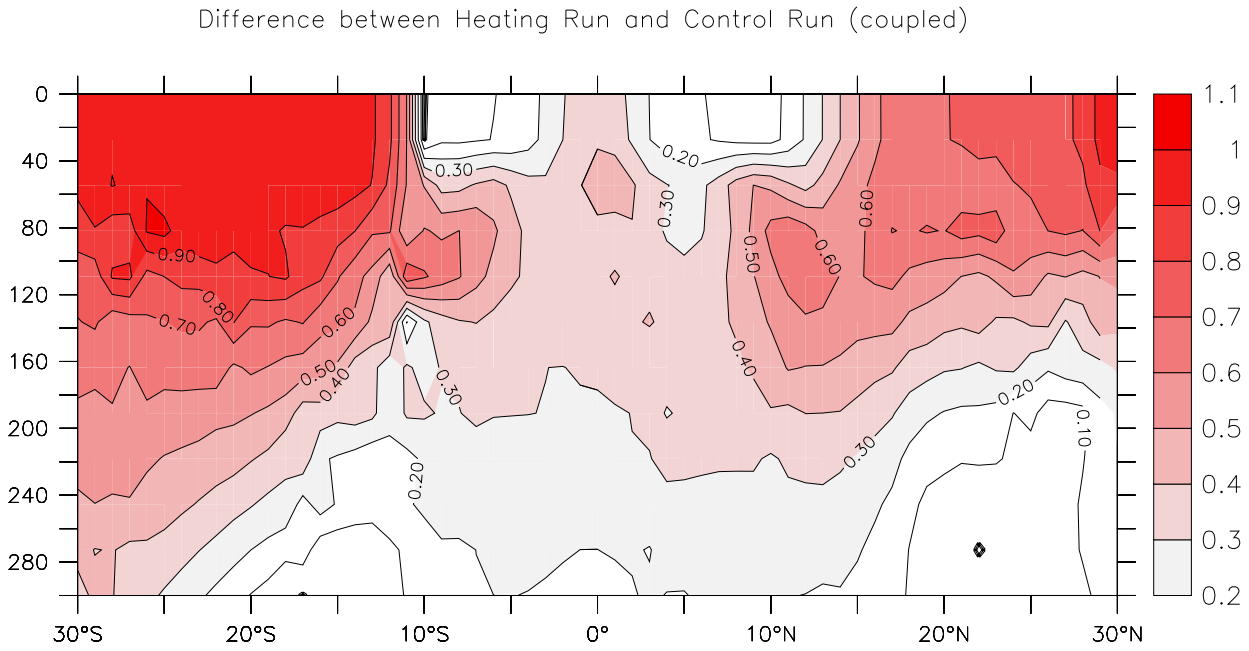

Figure 13 Depth–latitude section of temperature difference averaged from 90W to 150W (in C) between extra–tropical heating runand the control run without ENSO (a) and between the extra–tropical heating run and the control run with ENSO (b). The data used are the same as for Fig. 7.